



Published in final edited form as:

Bioorg Med Chem Lett. 2016 October 1; 26(19): 4857–4860. doi:10.1016/j.bmcl.2016.07.078.

Radiosynthesis and preliminary PET evaluation of ^{18}F -labeled 2-(1-(3-fluorophenyl)-2-oxo-5-(pyrimidin-2-yl)-1,2-dihydropyridin-3-yl)benzotrile for imaging AMPA receptors

Gengyang Yuan^{a,b}, Graham B. Jones^a, Neil Vasdev^{b,*}, and Steven H. Liang^{b,*}

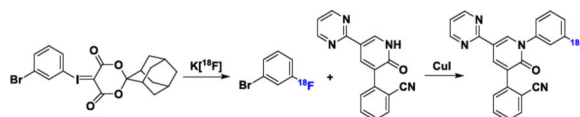
^aDepartment of Chemistry & Chemical Biology, Northeastern University, 360 Huntington Ave., Boston, MA 02115, USA

^bGordon Center for Medical Imaging & Division of Nuclear Medicine and Molecular Imaging, Massachusetts General Hospital and Department of Radiology, Harvard Medical School, 55 Fruit St., Boston, MA 02114, USA

Abstract

To prompt the development of ^{18}F -labeled positron emission tomography (PET) tracers for the α -amino-3-hydroxy-5-methyl-4-isoxazolepropionic acid (AMPA) receptor, we have prepared ^{18}F -labeled 2-(1-(3-fluorophenyl)-2-oxo-5-(pyrimidin-2-yl)-1,2-dihydropyridin-3-yl)benzotrile ($[^{18}\text{F}]\mathbf{8}$). The radiosynthesis was achieved by a one-pot two-step method that utilized a spirocyclic hypervalent iodine (III) mediated radiofluorination to prepare the ^{18}F -labeled 1-bromo-3-fluorobenzene ($[^{18}\text{F}]\mathbf{15}$) intermediate with K^{18}F . A subsequent copper (I) iodide mediated coupling reaction was carried out with 2-(2-oxo-5-(pyrimidin-2-yl)-1,2-dihydropyridin-3-yl)benzotrile ($\mathbf{10}$) to $[^{18}\text{F}]\mathbf{8}$ in $10 \pm 2\%$ uncorrected radiochemical yield relative to starting ^{18}F -fluoride with $> 99\%$ radiochemical purity and 0.8 ± 0.2 Ci/ μmol specific activity at the end of synthesis. PET imaging studies with the title radiotracer in normal mice demonstrated good brain uptake (peak standardized uptake value (SUV) = 2.3 ± 0.1) and warrants further *in vivo* validation.

Graphical Abstract



Keywords

AMPA receptor; Positron emission tomography; Fluorine-18; Radiotracer; Perampanel

*Corresponding author. Dr. Neil Vasdev, Tel.: +1-617-643-4736; vasdev.neil@mgh.harvard.edu; Dr. Steven H. Liang, Tel.: +1-617-726-6107; liang.steven@mgh.harvard.edu.

Publisher's Disclaimer: This is a PDF file of an unedited manuscript that has been accepted for publication. As a service to our customers we are providing this early version of the manuscript. The manuscript will undergo copyediting, typesetting, and review of the resulting proof before it is published in its final citable form. Please note that during the production process errors may be discovered which could affect the content, and all legal disclaimers that apply to the journal pertain.

Glutamate has been recognized as a principle excitatory neurotransmitter in the brain since late 1970s.¹ It exerts postsynaptic effects primarily through the metabotropic and ionotropic glutamate receptors (mGluRs and iGluRs, respectively).² The iGluRs structurally incorporate ligand-gated tetrameric ion channels and allow fast synaptic responses to the glutamate. The iGluRs are composed of three families, namely, N-methyl-D-aspartate (NMDA), kainite, and α -amino-3-hydroxy-5-methyl-4-isoxazolepropionic acid (AMPA) receptors.^{3–6} Modulation of these receptors can be used in the treatment of psychiatric disorders and neurodegenerative diseases, including epilepsy, ischemia, stroke, Parkinson's disease and Alzheimer's disease.^{7–8} In particular, competitive AMPA receptor antagonists have been the focus of drug discovery, with the first reported compound, 2, 3-dihydroxy-6-nitro-7-sulfamoylbenzo[f]quinoxaline-2, 3-dione (NBQX), in 1991,^{9–10} which led to the two clinically translated drugs, namely, Becampanel (AMP397) and Selurampanel (BGG492).^{11–12} To date, there has not been an AMPA receptor antagonist in this class of compounds to reach the market. Meanwhile, non-competitive AMPA receptor antagonists, which occupy the less polar allosteric binding site, are not expected to be significantly influenced by endogenous glutamate levels, as compared to the competitive antagonists.^{13–14} In this category, Talampanel (GYKI-537773) was studied in a Phase II clinical trial as an antiepileptic agent.^{15–16} Irampanel (BIIR561) reached Phase I/IIa clinical trials for the treatment of stroke.¹⁷ Perampanel (Fycompa[®]) has been approved by the United States Food and Drug Administration for treating refractory partial onset seizures in 2012, and as an adjunctive treatment for primary generalized tonic-clonic seizures in 2015.^{18–21}

As a non-invasive imaging technology, positron emission tomography (PET) is capable of *in vivo* quantification of biochemical and pharmacological progress via radiolabeled targeted molecular probes. Quantification of AMPA in the living brain by PET would enable investigations of the AMPA system under normal and disease conditions, assessment of AMPA distribution in the brain and periphery, and target engagement for validation of promising drug candidates in clinical trials. To date, only a handful of AMPA PET radiotracers, most of which are ¹¹C-labeled molecules, have been reported (Fig. 1). The radiosyntheses of isoquinoline derivatives [¹¹C]**1**, [¹⁸F]**2** and ¹¹C-labeled Perampanel ([¹¹C]**4**) have been reported, but their potential as PET tracers needs to be further evaluated *in vivo*.^{22–23} The isoquinoline derivative [¹¹C]**3**, showed rapid clearance from the central nervous system (CNS) and low specific binding in rats.²⁴ Among the recently disclosed PET tracers [¹¹C]**5–8** and [¹⁸F]**9**, [¹¹C]**5** and [¹¹C]**7** showed very low brain penetration in rhesus monkey (i.e. standardized uptake value (SUV)_{max} = 0.5), and [¹⁸F]**9** exhibited inconsistent distribution with the localization of AMPA receptors in rat brain. Whereas, [¹¹C]**6** demonstrated good radioactivity uptake in both rat and monkey brains (i.e. SUV_{max} = 1.6), consistent binding patterns with the AMPA localization and target specific binding features, hence, this radiotracer shows potential as PET tracer for AMPA receptors. A fluorinated isoquinoline derivative [¹¹C]**8** was radiolabeled via [¹¹C]HCN, displayed even higher radioactivity uptake in rhesus monkey brain (i.e. SUV_{max} = 2.7), and maintained the promising properties demonstrated with [¹¹C]**6**.^{25–26} In combination with the advantages of fluorine-18 that are attributed to its longer half-life ($t_{1/2}$ = 109.7 min) compared with carbon-11 ($t_{1/2}$ = 20.4 min), the goal of the present work is to develop a practical method for the radiosynthesis of the ¹⁸F-labeled isotopologue of **8** for imaging AMPA receptors with

PET. Herein, we describe a novel one-pot two-step radiosynthesis of [^{18}F]**8**, enabled by a spirocyclic hypervalent iodine (III) activated radiofluorination of the non-activated arene, and subsequent CuI mediated cross coupling with 2-(2-oxo-5-(pyrimidin-2-yl)-1, 2-dihydropyridin-3-yl) benzonitrile **10**. We further report preliminary PET imaging studies with [^{18}F]**8** in mice.

Radiofluorination of non-activated arenes still represents a challenging problem, despite extensive efforts devoted to this field.^{27–31} Unsurprisingly, attempts to achieve conventional nucleophilic aromatic substitution of the electron-deficient 2-(1-(3-nitrophenyl)-2-oxo-5-(pyrimidin-2-yl)-1, 2-dihydropyridin-3-yl)benzonitrile **11** (Scheme S1, Supporting Information, SI) with $\text{K}[^{18}\text{F}]$ or [^{18}F]tetraethylammonium fluoride ($\text{TEA}[^{18}\text{F}]$) led to no reaction.^{32,26} These results led us to utilize our recent developed radiofluorination method, which takes advantage of spirocyclic hypervalent iodine (III) species as the ^{18}F -radiolabeling precursors.^{33–37} To prepare the precursor for radiofluorination, aryl iodide **12** was first converted to the hypervalent spirocyclic iodine (III) compound, **13**, under oxidative conditions, and subsequently reacted with (1*r*,3*r*,5*r*,7*r*)-spiro[adamantane-2,2'-[1,3]dioxane]-4',6'-dione (SPIAD; **14**) (Scheme S2, SI).³⁷ Compound **10** was obtained from the coupling reactions between *N*-Boc-protected compound **17**, derived from compound **16**, and 2-cyanophenylboronic acid 1, 3-propanediol ester (**18**) under modified Ullmann reactions (Scheme S2, SI).²⁶

Our initial studies established the feasibility for our radiosynthetic approach for [^{18}F]**8** with coupling reactions between compound **10** and 1-bromo-3-fluorobenzene **15** (Scheme 1 and Scheme S3, SI). As shown in Step 1, Table 1, optimization of the radiofluorination of the iodine(III) precursor **13**, was carried out to yield [^{18}F]**15**. Compound [^{18}F]**15** was obtained in $72 \pm 3\%$ ($n > 10$) radiochemical conversion (RCC) under the optimal conditions, where compound **13** (3.9 μmol), K_2CO_3 (7.2 μmol), and K222 (Kryptofix[®], 13.3 μmol) were heated for 10 min at 120 °C in *N,N*-dimethylmethanamide (DMF, 0.2 mL) (Scheme S4 and Table S1, entries 4, SI).

The CuI mediated cross coupling (c.f. step 2) between compound **10** and [^{18}F]**15** was initially optimized based on the amount of compound **13** (2 mg, Table S1, entry 4, SI). *trans*-*N,N'*-dimethylcyclohexane-1, 2-diamine was an effective amine ligand to accomplish this coupling (Table 1, entry 1). Exploration of amine ligands, including *N,N,N',N'*-tetramethylethylenediamine (TMEDA), *N,N'*-dimethylethylenediamine (DMEDA) failed to produce [^{18}F]**8** (Table S2, entries 1–4, SI). Further optimization of reaction temperature (Table S2, entries 4–6, SI), stoichiometries of the coupling counterpart **10** (Table 1, entries 2–3 & Table S2, entries 7–9, SI), copper (I) iodide, its chelating amine and K_3PO_4 additive were carried out (Table 1, entries 4–6 & Table S2, entries 10–15, SI) to result in the ^{18}F -incorporation yield up to $72 \pm 5\%$ (Table 1, entry 5). To our surprise, the above-mentioned optimized reaction conditions resulted in low isolated radiochemical yield (RCY) non-decay-corrected relative to starting ^{18}F -fluoride (i.e. $\text{RCY} < 3\%$). In order to improve the RCY, the amounts of reagents involved in both steps were scaled up by 3-fold (i.e. 6 mg of compound **13**) and the 2nd step reaction was prolonged to 20 minutes. As a result, the corresponding isolated RCY of [^{18}F]**8** was significantly improved to $10 \pm 2\%$ after a 60 minute synthesis time ($n = 5$).

To determine the *in vivo* distribution and brain permeability of [¹⁸F]**8**, we performed preliminary PET imaging studies in mice. Administration of [¹⁸F]**8** in 10% ethanolic saline (0.4 mCi radioactivity, > 99% radiochemical purity (Fig. S1 & S2, SI), and specific activity of 0.8 ± 0.2 Ci/ μ mol (Fig. S3) at the time of injection) was coincident with initiation of 60 minute dynamic brain PET scans to determine biodistribution. As shown in Figure 2, [¹⁸F]**8** rapidly crossed the blood-brain barrier (BBB) and reached a maximum whole brain activity of 2.3 ± 0.1 SUV at approximately 70 seconds post injection of [¹⁸F]**8** (Fig. 2A). This result is consistent with the reported ¹¹C-isotopologue of **8**, confirming similar brain permeability of the [¹⁸F]**8**. We also determined the $\log P_{7.4}$ of compound **8** to be 1.5 by an established HPLC method,³⁸ which is similar to the experimental result of 1.7 in the report (Table S3 and Fig. S4, SI).²⁶ Further whole body biodistribution analysis revealed high uptake (SUV > 1) in the blood, heart, lung, kidney and liver at 1 min post injection, but low uptake in muscle and bladder over the entire analysis. The activity washed out rapidly from blood, heart and lung within 3 min, but slowly declined in kidney and liver over 60 min (Fig. 1B and Fig. S5A, SI).

In summary, we have synthesized the [¹⁸F]**8** via a novel one-pot two-step reaction, starting from a spirocyclic hypervalent iodine (III) precursor **13**, followed by a copper mediated *N*-arylation reaction. Preclinical PET imaging studies of [¹⁸F]**8** demonstrated consistent high brain uptake as its ¹¹C-isotopologue and showed reasonable uptake and clearance of activity in main organs, thereby representing a promising fluorine-18 labeled radiotracer for further evaluation as a potential AMPA receptor imaging agent.

Supplementary Material

Refer to Web version on PubMed Central for supplementary material.

Acknowledgments

We would like to thank the staff at the radiochemistry program, Gordon Center for Medical Imaging, Nuclear Medicine and Molecular Imaging, Massachusetts General Hospital, MA, and Department of Chemistry & Chemical Biology, Northeastern University for their generous support. We also thank Drs. Lee Collier, Benjamin H. Rotstein and Chongzhao Ran, Mr. Jian Yang and Ms. Jing Yang for their helpful discussions. S.H.L is a recipient of NIH career development award from the National Institute on Drug Abuse (DA038000).

Abbreviations

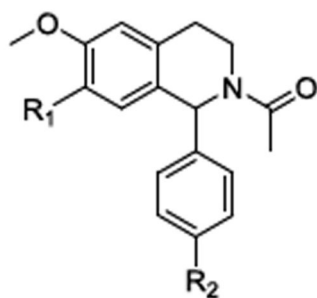
mGluRs	metabotropic glutamate receptors
iGluRs	ionotropic glutamate receptors
NMDA	<i>N</i> -methyl-D-aspartate
AMPA	α -amino-3-hydroxy-5-methyl-4-isoxazolepropionic acid
PET	positron emission tomography
CNS	central nervous system
TEA[¹⁸F]	[¹⁸ F]tetraethylammonium fluoride

SPIAD	(1 <i>r</i> ,3 <i>r</i> ,5 <i>r</i> ,7 <i>r</i>)-spiro[adamantane-2,2'-[1,3]dioxane]-4',6'-dione
RCC	radiochemical conversion
K₂₂₂	Kryptofix [®] or 4,7,13,16,21,24-Hexaoxa-1,10-diazabicyclo[8.8.8]hexacosanein
DMF	<i>N,N</i> -Dimethylmethanamide
TMEDA	<i>N,N,N',N'</i> -tetramethylethylenediamine
DMEDA	<i>N,N'</i> -Dimethylethylenediamine
TEAB	tetraethylammonium bicarbonate
SUV	standardized uptake value
RCY	radiochemical yield
DMSO	Dimethyl sulfoxide
BBB	crossed the blood-brain barrier
TAC	Time-activity curve
ROI	region of interest

References and notes

- Meldrum BS. *J. Nutr.* 2000; 130:1007S. [PubMed: 10736372]
- Niswender CM, Conn PJ. *Annu. Rev. Pharmacool. Toxicol.* 2010; 50:295.
- Mayer ML, Armstrong N. *Annu. Rev. Physiol.* 2004; 66:161. [PubMed: 14977400]
- Watkins JC, Jane DE. *Brit. J. Pharmacol.* 2006; 147:S100. [PubMed: 16402093]
- Traynelis SF, Wollmuth LP, McBain CJ, Menniti FS, Vance KM, Ogden KK, Hansen KB, Yuan HJ, Myers SJ, Dingledine R. *Pharmacol. Rev.* 2010; 62:405. [PubMed: 20716669]
- Kew JNC, Kemp JA. *Psychopharmacology.* 2005; 182:320.
- Calabresi P, Cupini LM, Centonze D, Pisani F, Bernardi G. *Ann. Neurol.* 2003; 53:693. [PubMed: 12783414]
- Chang PKY, Verbich D, McKinney RA. *Eur. J. Neurosci.* 2012; 35:1908. [PubMed: 22708602]
- Klockgether T, Turski L, Honore T, Zhang ZM, Gash DM, Kurlan R, Greenamyre JT. *Ann. Neurol.* 1991; 30:717. [PubMed: 1662477]
- Meldrum BS, Rogawski MA. *Neurotherapeutics : the journal of the American Society for Experimental NeuroTherapeutics.* 2007; 4:18. [PubMed: 17199015]
- Ornstein PL, Arnold MB, Augenstein NK, Lodge D, Leander JD, Schoepp DD. *J. Med. Chem.* 1993; 36:2046. [PubMed: 8393116]
- Faught E. *Expert Opin. Inv. Drug.* 2014; 23:107.
- Barreca ML, Gitto R, Quartarone S, De Luca L, De Sarro G, Chimirri A. *J. Chem. Inf. Comp. Sci.* 2003; 43:651.
- Balannik V, Menniti FS, Paternain AV, Lerma J, Stern-Bach Y. *Neuron.* 2005; 48:279. [PubMed: 16242408]
- Donevan SD, Yamaguchi S, Rogawski MA. *J. Pharmacol. Exp. Ther.* 1994; 271:25. [PubMed: 7525924]
- Chappell AS, Sander JW, Brodie MJ, Chadwick D, Lledo A, Zhang D, Bjerke J, Kiesler GM, Arroyo S. *Neurology.* 2002; 58:1680. [PubMed: 12058100]

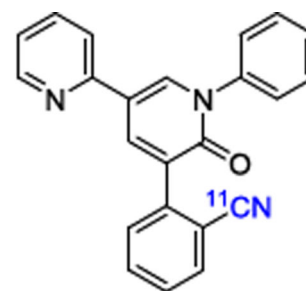
17. Feigin V. *Curr. Opin. Investig. Drugs*. 2002; 3:908.
18. Hanada T, Hashizume Y, Tokuhara N, Takenaka O, Kohmura N, Ogasawara A, Hatakeyama S, Ohgoh M, Ueno M, Nishizawa Y. *Epilepsia*. 2011; 52:1331. [PubMed: 21635236]
19. Hibi S, Ueno K, Nagato S, Kawano K, Ito K, Norimine Y, Takenaka O, Hanada T, Yonaga M. *J. Med. Chem.* 2012; 55:10584. [PubMed: 23181587]
20. French JA, Krauss GL, Steinhoff BJ, Squillacote D, Yang HC, Kumar D, Laurenza A. *Epilepsia*. 2013; 54:117. [PubMed: 22905857]
21. French JA, Krauss GL, Wechsler RT, Wang XF, DiVentura B, Brandt C, Trinka E, O'Brien TJ, Laurenza A, Patten A, Bibbiani F. *Neurology*. 2015; 85:950. [PubMed: 26296511]
22. Gao M, Kong D, Clearfield A, Zheng QH. *Bioorg. Med. Chem. Lett.* 2006; 16:2229. [PubMed: 16455250]
23. Lee HG, Milner PJ, Placzek MS, Buchwald SL, Hooker JM. *J. Am. Chem. Soc.* 2015; 137:648. [PubMed: 25565277]
24. Arstad E, Gitto R, Chimirri A, Caruso R, Constanti A, Turton D, Hume SP, Ahmad R, Pilowsky LS, Luthra SK. *Bioorg. Med. Chem.* 2006; 14:4712. [PubMed: 16621575]
25. Oi, N.; Yamamoto, N.; Suzuki, M.; Nakatani, Y.; Suhara, T.; Zhang, M-R.; Fukumura, T.; Higuchi, M.; Minamimoto, T.; Maeda, J.; Tokunaga, M.; Nagai, Y. WO2014143210 A1. 2014.
26. Oi N, Tokunaga M, Suzuki M, Nagai Y, Nakatani Y, Yamamoto N, Maeda J, Minamimoto T, Zhang MR, Suhara T, Higuchi M. *J. Med. Chem.* 2015; 58:8444. [PubMed: 26469379]
27. Preshlock S, Tredwell M, Gouverneur V. *Chem. Rev.* 2016; 116:719. [PubMed: 26751274]
28. Tredwell M, Gouverneur V. *Angew. Chem. Int. Ed. Engl.* 2012; 51:11426. [PubMed: 23086547]
29. Brooks AF, Topczewski JJ, Ichiishi N, Sanford MS, Scott PJ. *Chem. Sci.* 2014; 5:4545. [PubMed: 25379166]
30. Campbell MG, Ritter T. *Chem. Rev.* 2015; 115:612. [PubMed: 25474722]
31. Buckingham F, Gouverneur V. *Chem. Sci.* 2016; 7:1645.
32. Terence, S. WO03047577A2. 2003.
33. Rotstein BH, Stephenson NA, Vasdev N, Liang SH. *Nat. Commun.* 2014; 5:4365. [PubMed: 25007318]
34. Stephenson NA, Holland JP, Kassenbrock A, Yokell DL, Livni E, Liang SH, Vasdev N. *J. Nucl. Med.* 2015; 56:489. [PubMed: 25655630]
35. Jacobson O, Weiss ID, Wang L, Wang Z, Yang X, Dewhurst A, Ma Y, Zhu G, Niu G, Kiesewetter DO, Vasdev N, Liang SH, Chen X. *J. Nucl. Med.* 2015; 56:1780. [PubMed: 26315836]
36. Wang L, Jacobson O, Avdic D, Rotstein BH, Weiss ID, Collier L, Chen X, Vasdev N, Liang SH. *Angew. Chem. Int. Ed. Engl.* 2015; 54:12777. [PubMed: 26308650]
37. Rotstein BH, Wang L, Liu RY, Patteson J, Kwan EE, Vasdev N, Liang SH. *Chem. Sci.* 2016; 7:4407. [PubMed: 27540460]
38. Webster GRB, Friesen KJ, Sarna LP, Muir DCG. *Chemosphere*. 1985; 14:12.



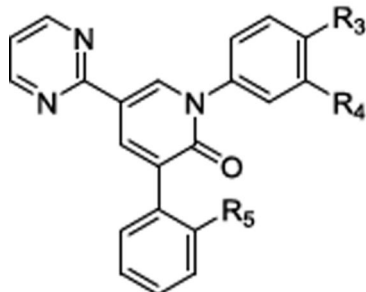
[¹¹C]1, R₁=OCH₃, R₂=**[¹¹C]OCH₃**

[¹⁸F]2, R₁=OCH₃, R₂=**[¹⁸F]F**

[¹¹C]3, R₁=**[¹¹C]OCH₃**, R₂=Cl



[¹¹C]4 (Perampanel)



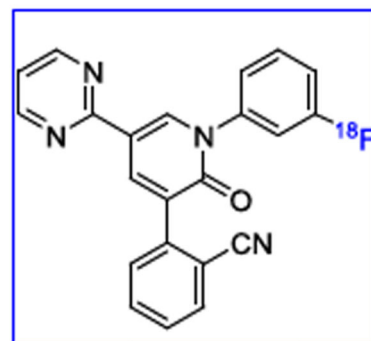
[¹¹C]5, R₃=H, R₄=NH₂, R₅=**[¹¹C]CN**

[¹¹C]6, R₃=H, R₄=**[¹¹C]NHCH₃**, R₅=CN

[¹¹C]7, R₃=F, R₄=NH₂, R₅=**[¹¹C]CN**

[¹¹C]8, R₃=H, R₄=F, R₅=**[¹¹C]CN**

[¹⁸F]9, R₃=H, R₄=**[¹⁸F]CH₂F**, R₅=F



[¹⁸F]8

Figure 1.
Chemical Structures of the reported PET tracers for AMPA receptors.

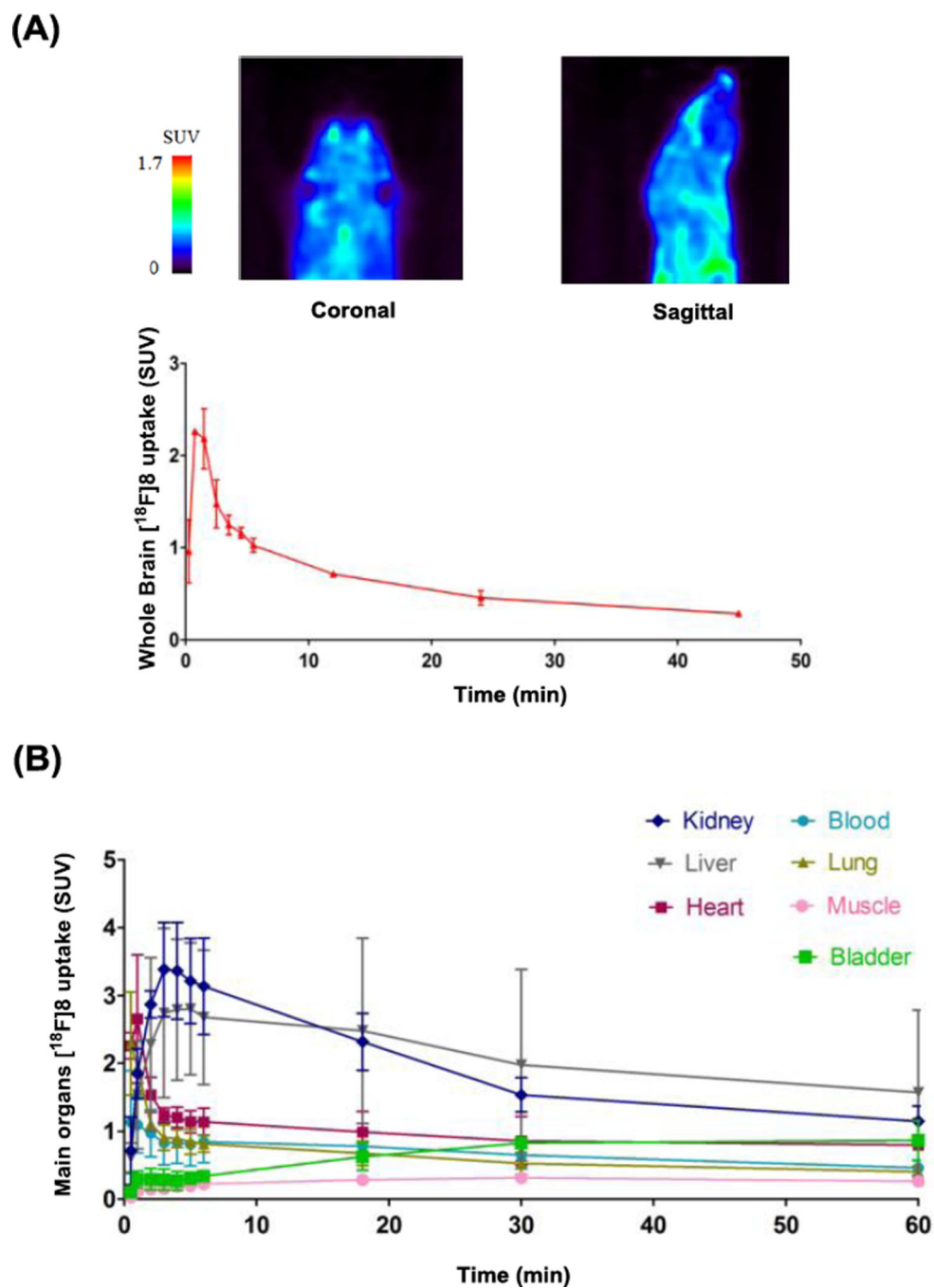
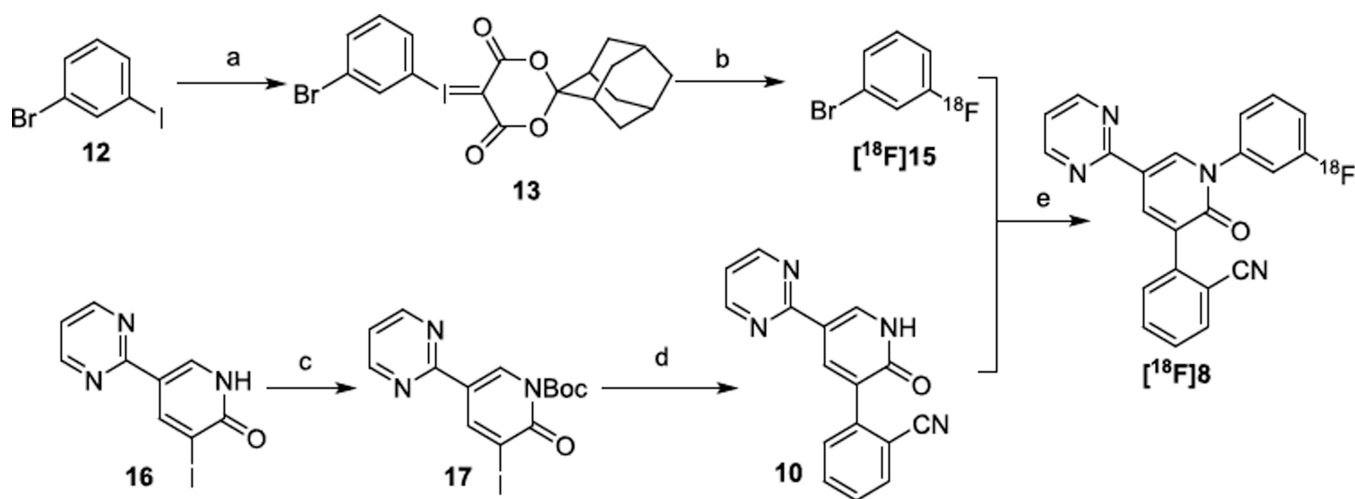


Figure 2. PET imaging of [¹⁸F]8 in mice: (A) Summed image 0–60 min post tracer injection in the brain. (B) Time-activity curves (TACs) of whole body biodistribution. Data are expressed as SUV (mean ± SD, n = 2). For region of interest (ROI) placement, see supporting information (Figure S5A, SI).



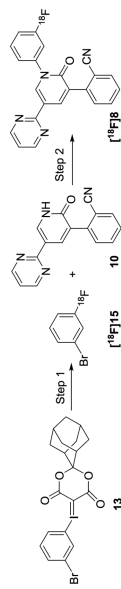
Scheme 1.

De novo radiosynthesis of [18F]8a.

^aReagents and conditions: (a) (i) NaBO₃·4H₂O, glacial acetic acid, 50 °C, Overnight; (ii) (1*r*, 3*r*,5*r*,7*r*)-spiro[adamantane-2,2'-[1,3]dioxane]-4',6'-dione (SPIAD) **14**, 10% Na₂CO₃ (aq) (w/v), ethanol/dichloromethane; (b) K[¹⁸F] or TEA[¹⁸F], DMF, 120 °C, 10 min. (c) di-*tert*-butyl dicarbonate, 4-dimethylaminopyridine, THF, 0 °C to room temperature, Overnight; (d) 2-cyanophenylboronic acid 1,3-propanediol ester **18**, Cesium carbonate, Pd(PPh₃)₄, DMF, 110 °C, overnight. (e) CuI, K₃PO₄, *trans*-*N,N'*-dimethylcyclohexane-1, 2-diamine, DMF, 110 °C, 20 min.

Table 1

Optimization of reaction conditions for the synthesis of [¹⁸F]8



Entry ^a	10 (mg)	CuI (mg)	Amine (μL) ^c	K ₃ PO ₄ (mg)	T (°C)	Time (min)	DMF (mL)	[¹⁸ F]8 (%) ^d
1	2	2	1.2	4.8	110	10	0.4	8 ± 4 (n = 2)
2	4	2	1.2	4.8	130	10	0.4	20 ± 3 (n = 2)
3	16	2	1.2	4.8	130	10	0.4	6 ± 3 (n = 2)
4	4	4	2.4	4.8	130	10	0.4	48 ± 5 (n = 2)
5	4	12	7.2	4.8	130	10	0.4	72 ± 5 (n = 5)
6	4	12	7.2	15	130	10	0.4	20 ± 1 (n = 2)
7 ^b	12	36	21.6	14.4	130	20	1.0	65 ± 10 (n = 5)

^aUnless otherwise noted, the step 1 reaction mixture was from Table S1, entry 4, SI.

^bThe step 1 reaction mixture was from Table S1, entry 13, SI.

^cAmine refers to trans-*N,N'*-dimethylcyclohexane-1,2-diamine.

^dDetermined by radio-HPLC integration of product peaks, relative to [¹⁸F]fluoride and ¹⁸F-side products if observed.